Influence of Salt on the Aqueous Lubrication Properties of End-Grafted, Ethylene Glycol-Based Self-Assembled Monolayers

Raphael Heeb, Seunghwan Lee, Nagaiyanallur V. Venkataraman, and Nicholas D. Spencer*

Laboratory for Surface Science and Technology, Department of Materials, ETH Zurich, Wolfgang-Pauli-Strasse 10, CH-8093 Zurich, Switzerland

ABSTRACT We have investigated the influence of a high-concentration salt solution (1 M NaCl) on the aqueous lubrication properties of ethylene glycol-based molecules, namely, α-methoxy-ω-mercaptopoly(ethylene glycol) (MW 5000 Da) and α-methoxy-ω-mercaptoheptakis(ethylene glycol) (MW 356 Da), which have been end-grafted onto polycrystalline gold surfaces at high surface density. Macroscopic-scale, yet nondestructive, pin-on-disk tribometry experiments revealed that a high concentration of sodium chloride is deleterious to the aqueous lubricating properties of both films under low-sliding-speed conditions. This behavior was observed to be closely associated with the more collapsed conformation of surface-grafted poly(ethylene glycol) polymer chains in concentrated salt solutions, as confirmed by quartz-crystal microbalance measurements.

KEYWORDS: aqueous lubrication • self-assembled monolayer (SAM) • poly(ethylene glycol) • salting out • poly(dimethylsiloxane)

INTRODUCTION

End-tethered polymer chains have drawn considerable attention in the past decade as an effective means to achieving ultralow interfacial friction (1−4). When two surfaces sliding past each other are modified with end-grafted polymer chains, the interfacial friction forces can be greatly reduced under "good" solvents. Under these conditions, the tethered polymer chains display a highly extended "brushlike" conformation, acting as a cushioning layer to sustain externally applied pressure. Thus, the solvent quality plays a critical role in determining the lubricity of such systems; when exposed to solvents with poor solvent quality, the polymer chains adopt a collapsed state, and thus the cushioning effect to withstand external pressure is correspondingly impaired. Previous studies have also shown that the lubricating effects of surface-grafted polymer chains are concomitantly degraded in liquids with poor solvent quality (5−11).

Lubrication by means of end-tethered polymers is particularly attractive for water-soluble polymers in an aqueous environment, opening the possibility of using water as a lubricant. In this regard, poly(ethylene glycol) (PEG) has been most intensively investigated (1, 4, 7, 8, 12−15), partly because of its unique solubility in water and partly because of its excellent biocompatibility (15−17). Many previous studies involving PEG polymer brushes have shown a great enhancement in the aqueous lubrication properties of various materials (1). One of the critical aqueous parameters that has been known to affect various PEG solution properties is the ionic strength; generally, the addition of a high concentration of electrolytes into aqueous PEG solutions is known to decrease the solubility of PEG by disrupting the unique ethylene glycol (EG)−water structure, i.e., by "salting-out" (18−23) and/or by complexation of PEG with cations (24, 25). This latter effect is similar to the ion complexation of crown ethers, where the cation is immobilized inside the polyether ring through ion-dipole interactions with ether O atoms (26). The ability of PEG to form complexes with cations stems from the high flexibility of the polyether chain, but the effect is considerably weaker than that observed with cyclic ethers (27). The "salting-out" effect of PEG is believed to arise from the disruption of structured water in the vicinity of the chain, which normally accounts for the stabilization of the helical PEG conformation in water. It has been reported that ions disturb the water structure around PEG chains by becoming hydrated (28). Both effects are known to induce a smaller radius of gyration of PEG chains, a reduced viscosity, and a lower cloud-point temperature (18−25). In other words, the addition of salts into aqueous PEG solutions results in degradation of the solvent quality of water toward PEG.

A similar salt effect, due to degrading solvent quality, would be expected for the aqueous lubricating properties of PEG chains that are end-grafted onto surfaces. However, a direct experimental correlation between the conformational change and the aqueous lubricating properties of the end-tethered PEG chains induced by the addition of salts has been scarcely addressed. The influence of the solvent quality on the lubricating properties of surface-grafted PEG chains has been investigated, in a general sense, by employing organic solvents that differ from water in their solvent quality (6−9). Challenges in obtaining the salt-effect data include the stringent experimental conditions that need to be met

* Corresponding author. E-mail: spencer@mat.ethz.ch.
Received for review January 30, 2009 and accepted April 13, 2009

DOI: 10.1021/am900062h

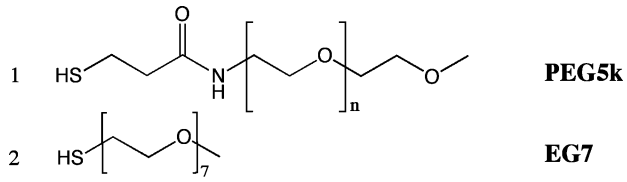

FIGURE 1. Molecular structure of thiol molecules from which SAMs were generated on polycrystalline Au substrates.

to investigate the influence of salts on the conformational change and the aqueous lubricating properties of surface-grafted PEG chains. First, anchoring of PEG chains should be stable enough to allow them to remain immobilized on the surface during the course of exposure to a high-salt aqueous solution. This restricts potential anchoring approaches for PEG chains to those that are immune to changes in electrostatic interactions between anchoring groups of polymer chains and the substrate, such as covalent bonding. For this reason, in this study we have selected PEG chains end-functionalized with thiol groups (−SH), namely, α-methoxy-ω-mercaptopoly(ethylene glycol) (MW 5000 Da), which can readily be bound onto gold (Au) surfaces (see Figure 1). For comparison purposes, an oligo(ethylene glycol) analogue, namely, α-methoxy-ω-mercaptoheptakis(ethylene glycol) (MW 356 Da), was also employed to investigate the role of the EG chain length in aqueous lubrication (see Figure 1). We have selected sodium chloride (NaCl) for its practical importance and its monovalence; we have selected 1 M as the concentration of NaCl because previous studies on bulk aqueous PEG solution properties have shown that a noticeable change is expected only in the high-concentration regime (28, 29).

For tribological tests, the tribostress should be mild enough as to not induce desorption of PEG chains from the surface; if grafted PEG chains are desorbed because of tribostress and then possibly readsorbed, the probed changes in frictional properties induced by changes in the solvent quality can be complicated by effects involving the (re)adsorption kinetics of the polymer chains (30). As is well-known, tribological testing with conventional pin-on-disk tribometry generally leads to a rapid and irreversible failure of most adsorbed monomolecular organic films because of high local contact pressures at the multiple-asperity contacts (31−33). However, by employing a soft rather than a rigid slider in a conventional pin-on-disk tribometer (34), nondestructive probing of the tribological properties of ultrathin organic films can be readily achieved by virtue of the elastic pin deformation and low contact pressure generated within the contact area. While nondestructive, mild tribocontacts can also be achieved by nanotribological approaches, such as atomic force microscopy (AFM) (35−41) or the surface forces apparatus (2, 5, 12, 13), the current approach has the distinct advantage that the regions of organic films within the contact area can be examined by spectroscopic approaches because of the large contact area between the pin and disk.

The tribometry setup described above, combined with the appropriate PEG immobilization chemistry, thus enables an investigation of the influence of salts on the aqueous lubrication properties of brushlike PEG layers. It is emphasized that, because of the immobilization of PEG chains by a method that is impervious to changes in the salt concentration and tribostress, the probed frictional properties can be entirely ascribed to the conformational changes of the surface-grafted PEG chains arising from salt effects. In parallel with tribological measurements, the structure and stability of the brushlike PEG layer have been probed by standard surface-analytical tools, including polarization−modulation infrared reflection−absorption spectroscopy (PM-IRRAS), variable-angle spectroscopic ellipsometry (VASE), and static contact angle measurements. The structural changes of the adsorbed polymer upon the addition of salt have been probed by quartz-crystal microbalance (QCM-D) and can be correlated with the aqueous lubrication properties.

EXPERIMENTAL METHODS

Preparation of Self-assembled Monolayers (SAMs) on Au. SAMs on Au substrates were generated through spontaneous adsorption of thiol-terminated EG molecules (Figure 1) from absolute ethanol (Fluka, Buchs, Switzerland). Monolayers of α-methoxy-ω-mercaptopoly(ethylene glycol) (MW 5000 Da; **1** in Figure 1) as well as α-methoxy-ω-mercaptoheptakis(ethylene glycol) (MW 356 Da; **2** in Figure 1) (Iris Biotech GmbH, Marktredwitz, Germany) were prepared as follows. Soda-lime glass slides (SuperFrost, Menzel-Gläser, Braunschweig, Germany) were cut into square pieces of 2.5 × 2.5 cm^2 and thoroughly cleaned by ultrasonication in ethanol, followed by air-plasma treatment (high power, Harrick Plasma Cleaner/Sterilizer, Ossining, NY). After thermal evaporation (MED020 coating system, BALTEC, Balzers, Liechtenstein) of 10 nm of Cr (adhesion layer) and 100 nm of Au, the substrates were immersed in 50 μM ethanolic thiol solutions for >24 h. All chemicals were used as received, without further purification.

In the following, the tested SAMs are abbreviated as shown in Figure 1: α-methoxy-ω-mercaptopoly(ethylene glycol) of 5000 Da (1) as **PEG5k** and α-methoxy-ω-mercaptoheptakis(ethylene glycol) (2) as **EG7**.

Fabrication of Poly(dimethylsiloxane) (PDMS) Pins. For macroscopic pin-on-disk experiments, hemispherical PDMS pins were fabricated by thoroughly mixing the base and curing agent of a two-component silicone elastomer kit (SYLGARD 184, Dow Corning, Midland, MI) in a 10:1 ratio by weight. After removal of the generated air bubbles by a gentle vacuum, the mixture was transferred into a cell-culture plate (96 MicroWell Plates NUNCLON Δ, Nunc A/S, Roskilde, Denmark) with round-bottomed wells of 6 mm diameter. Curing of the pins was carried out at 70 °C for 24 h.

In order to remove uncrosslinked, low-molecular-weight species such as fillers and unreacted siloxanes present within the PDMS network, the pins were immersed in *n*-hexane (96 % HPLC grade, Scharlau Chemie SA, Barcelona, Spain) for 24 h, and the solvent exchanged twice during this period. Subsequently, the swollen pins were dried in an evacuated desiccator for 1 h and stored in an ambient atmosphere for >24 h before use.

Prior to pin-on-disk experiments, the PDMS pins were air-plasma-treated for 60 s at a gas pressure of 0.1 Torr. The oxidized pins, referred to as **ox-PDMS** pins in the following, displayed a water contact angle of <3°, and they were employed in tribological measurements immediately after plasma treatment.

Pin-on-Disk Tribometry. The macroscopic sliding friction between **ox-PDMS** pins and SAM-bearing substrates was measured with a conventional pin-on-disk tribometer (CSM Instruments SA, Peseux, Switzerland). In this setup, the pin-bearing measuring arm is loaded by dead weights and brought into

contact with the rotating disk. The resulting frictional forces are obtained upon lateral deflection of the measuring arm via a strain gauge.

All experiments were conducted in two aqueous buffer solutions of varying salt concentration, namely, 1 mM 4-(2-hydroxyethyl)piperazine-1-ethanesulfonic acid (HEPES, BioChemika Ultra, Fluka, Buchs, Switzerland) in pure water (referred to as **HEPES 0**) and in its equivalent with 1 M sodium chloride (NaCl) (referred to as **HEPES 0, 1 M NaCl**). The frictional properties of the sliding contacts between the SAM films and **ox-PDMS** pins were initially characterized over a wide range of speeds (from 19 to 0.1 mm/s) under a load of 1 N. The coefficient of friction (μ) was recorded over 10 rotations (6 mm track radius) at eight different sliding speeds, and all measurements were performed on the same sliding track by gradually decreasing the linear speed from 19 to 0.1 mm/s. Although the sliding tracks for some tribopairs were discernible under an optical microscope, IR spectroscopy confirmed that the SAM films on Au were virtually intact after tribostress.

Contact-Angle Measurements. Prior to pin-on-disk measurements, static water contact angles of the SAM films were measured with the sessile-drop method employing a contact-angle goniometer (Ramé-Hart model 100, Ramé-Hart Instrument Co., Netcong, NJ). The contact angles were determined immediately after samples were taken out of the thiol solutions, thoroughly rinsed with ethanol and ultrapure water to remove unbound or loosely bound molecules, and blown dry with a N_2 gas stream. The static contact angles of at least five samples with identical surface chemistry were measured and averaged.

VASE. The film thicknesses of the adsorbed SAMs on Au in a dry state were characterized by ellipsometry (VASE, M-2000F, LOT Oriel GmbH, Darmstadt, Germany) at three different angles of incidence (65°, 70°, and 75°). The measured data were fitted with the analysis software provided by the manufacturer (WVASE32, LOT Oriel GmbH, Darmstadt, Germany), and the spectral range considered was from 370 to 995 nm. The dry film thickness of the organic top layer with an assumed refractive index of 1.45 was extracted from the analysis of a three-layer model.

PM-IRRAS. The structural properties of the two different SAMs on Au were analyzed by PM-IRRAS using a Bruker IFS 66v IR spectrometer (Bruker Optik GmbH, Ettlingen, Germany) with a photoelastic modulator (PMA 37, Bruker Optik GmbH, Ettlingen, Germany). The infrared beam from the external beam port was passed through a KRS-5 wire-grid polarizer and a photoelastic modulator. Thereafter, the incident beam was reflected at the sample surface at an angle of 80° and detected with an N_2(l)-cooled MCT detector. For all measurements, 1024 scans were collected with an 8-cm^{-1} resolution. The multiplexed interferograms were processed and baseline-corrected with a polynomial using the instrument software (OPUS, Bruker Optik GmbH, Ettlingen, Germany).

PM-IRRA spectra of the substrates were first recorded after >24 h of thiol self-assembly. In order to test the stability of the SAMs in lubricants (under no tribostress), IR spectra were further recorded after 2 h of immersion of the samples into the two lubricants employed in this work, where the immersion time corresponded to the duration of a pin-on-disk measurement.

QCM with Dissipation Monitoring (QCM-D). In order to gain specific insight into the conformation of the surface-anchored long-chain PEG thiols (**PEG5k**) and the related lubrication mechanism, QCM-D experiments were performed (Q-Sense E4, Q-Sense AB, Västra Frölunda, Sweden). The detailed working principle of the QCM-D is described elsewhere (42, 43). Briefly, this highly sensitive weighing device measures changes in the resonance frequency of a piezoelectric quartz crystal upon mass change (e.g., adsorption of molecules on the surface) as well as the total energy dissipation D (damping) of the resonator after the driving voltage is switched off. The dissipation D represents the sum of all energy losses per oscillation cycle and is therefore very sensitive to the viscoelastic properties of the adlayer. Hence, QCM-D represents an appropriate technique for structural investigations of polymer brushes in aqueous environments.

Table 1. Static Water Contact Angles and Ellipsometric Dry Thicknesses of the Employed Thiol SAMs

	CA_{H_2O} (deg)	d_{ELM} (nm)
PEG5k	30 ± 1	8.22 ± 1.77
EG7	69 ± 1	2.06 ± 0.04
Au	82 ± 2	

After 4 h of in situ adsorption of **PEG5k** SAMs from a 50 μM ethanolic solution on the Au-coated quartz crystal, the cell was flushed with ethanol to remove unbound thiol molecules. Subsequently, **HEPES 0** was injected in order to reflect the environment encountered by the **PEG5k** SAM during aqueous lubrication. Thereafter, the low-salt aqueous solution was replaced with **HEPES 0, 1 M NaCl** in order to investigate variations in the mass and structural properties (i.e., hydration) of the films at higher salt concentrations.

RESULTS AND DISCUSSION

A. Sample Characterization Prior to Tribological Experiments. In order to verify the SAM formation on Au, the samples were characterized by various surface-analytical tools prior to pin-on-disk experiments. The average static water contact angles from at least five samples are summarized in Table 1.

They were determined to be 30 ± 1° for **PEG5k** and 69 ± 1° for **EG7**, whereas the bare Au substrates exhibited a water contact angle of 82 ± 2°. The distinctively lower water contact angles of the **PEG5k** SAMs compared to the bare Au substrates are consistent with the predominant exposure of hydrophilic moieties on the surface. The **EG7** monolayers revealed a significantly higher water contact angle compared to their long-chain analogues (**PEG5k**). It was previously reported that thiolated oligo(ethylene glycol) SAMs adopt a well-ordered 7/2 helical structure on polycrystalline Au surfaces (44, 45). Thus, the water contact angle observed on **EG7** SAMs, which is more than 2 times higher than that obtained from **PEG5k** SAMs, could be a consequence of the predominant exposure of terminal methoxy groups to the surface in helically ordered **EG7** SAMs compared to their random-coiled, long-chain analogues (**PEG5k**), which can expose the ether O atoms.

The dry film thicknesses of the SAMs on Au substrates measured by ellipsometry were found to be 8.22 ± 1.77 nm for **PEG5k** and 2.06 ± 0.04 nm for **EG7**, as shown in Table 1. The values are averaged over a minimum of five samples. The large error bar in the **PEG5k** thickness values can be attributed to the slightly fluctuating room temperature, which was shown to be very close to the cloud point of 50 μM **PEG5k** thiol solutions in ethanol. According to a model proposed by Sofia et al. (15), the dry thickness values obtained from ellipsometry measurements can be converted into an approximate surface grafting density.

As shown in the two-dimensional illustration in Figure 2, the definition of a unit cell (side lengths L and height d) for

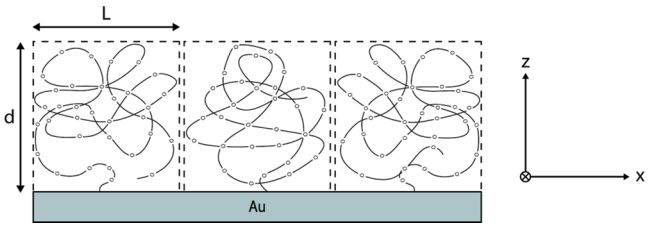

FIGURE 2. Two-dimensional schematic of close-packed unit cells, each bearing one polymer chain, for the derivation of the surface grafting density.

each chain attached to the surface allows for the calculation of the volume V occupied by a single chain through

$$V = L^2 d = \frac{M_w}{\rho_{dry} N_A} \quad (1)$$

where L^2 is the surface area occupied by a single chain, d is the dry thickness measured by ellipsometry, M_w is the molecular weight of the PEG chains, ρ_{dry} is the density of the dry monolayer, and N_A is Avogadro's number. The surface grafting density, i.e., the number of attached chains per unit area, can then be expressed as

$$\frac{1}{L^2} = \frac{d\rho_{dry} N_A}{M_w} \quad (2)$$

In eqs 1 and 2, a constant value for the dry density of the monolayer (ρ_{dry}) has to be assumed; i.e., close packing of attached chains on the surface is a prerequisite for the validity of this model. Assuming a value of 1 g/cm^3 for the density of the dry PEG monolayer, the calculated surface density of the **PEG5k** SAMs was determined to be 1.02 ± 0.22 chains/nm^2. This value is substantially higher than the previously reported grafting density of 5 kDa PEG monolayers adsorbed from aqueous solutions (46). We attribute the higher dry thickness of our monolayers to the poor solubility of PEG in ethanol as opposed to aqueous solutions, which tends to induce a smaller radius of gyration of PEG chains in bulk solution and, in turn, facilitates a denser packing on the surface. This value is still much lower than the calculated close-packed all-trans surface density of **PEG5k** SAMs on Au (5.88 chains/nm^2) (46), indicating a considerable degree of disorder within the **PEG5k** monolayers. In comparison, the surface density of **EG7** SAMs was found to be 3.49 ± 0.06 chains/nm^2 and implies a more ordered structure of the short EG-based monolayers. Vanderah et al. have calculated the theoretical thickness of oligo(ethylene glycol) thiols with different structural conformations (44, 45). According to these authors, the expected all-trans thickness of **EG7** SAMs would be 2.85 nm. In contrast, the 7/2 helical conformation of **EG7** SAMs would result in a theoretical thickness of 2.27 nm, which is equivalent to 3.84 chains/nm^2. Our results, with average thickness values of 2.06 nm and a corresponding surface grafting density of 3.49 ± 0.06 chains/nm^2, thus suggest that **EG7** SAMs exhibit a predominantly helical conformation.

IR spectroscopy was employed to characterize the compositional and structural features of the SAM films on Au as well as to study the film stability after exposure to aqueous lubricants. PM-IRRA spectra obtained after thiol adsorption revealed the successful formation of SAMs from both thiols. Figure 3 shows the PM-IRRA spectra recorded from the two EG-based monolayers, and the corresponding assignments of the peaks are summarized in Table 2. The spectra are normalized to ellipsometric thickness to afford a better comparison of the relative intensities in the two spectra.

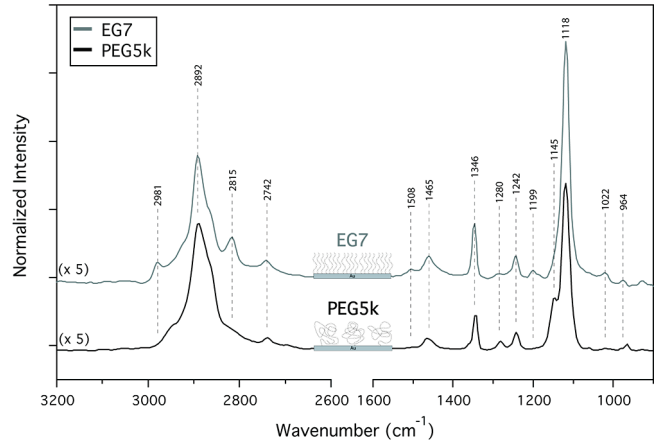

FIGURE 3. PM-IRRA spectra recorded from EG-based SAMs (PEG5k and EG7) prior to pin-on-disk tribometry.

Table 2. Assignment of Peaks from PM-IRRAS Spectra Recorded for EG7 and PEG5k SAMs

EG7 (cm^{-1})	**PEG5k** (cm^{-1})	assignment
2981		CH_3 asym. str.
2892	2889	CH_2 sym. str.
2815		CH_3 sym. str.
2742	2742	CH_2 combination
1508		
1461	1465	CH_2 scissoring
1346	1346	CH_2 wagging
1284	1280	CH_2 twisting
1242	1242	CH_2 twisting
1199		CH_3 rocking
	1145	C−O−C str. (trans)
1118	1118	C−O−C str. (helical)
1022		
975	964	CH_2 rocking

Both **PEG5k** and **EG7** exhibit strong bands in the high-frequency (3100−2700 cm^{-1}) region, arising from the C−H stretching modes, and in the low-frequency (1500−900 cm^{-1}) regions, due to the CH_2 bending and the C−O and C−C stretching modes. The bands at 1347, 1243, and 965 cm^{-1} are assigned to the $-CH_2-$ wagging, twisting, and rocking modes, respectively. The strong band at 1118 cm^{-1} is assigned to the C−O−C stretching mode. The positions of these bands in **EG7** SAMs are similar to those reported for the ordered helical structure of the oligo(ethylene glycol) SAMs (44). The spectrum obtained from **PEG5k** monolayers is similar to that from **EG7** SAMs, yet with some important differences. In the **EG7** case, the C−O−C stretching band appears as a single peak with a maximum at 1118 cm^{-1}, whereas in the **PEG5k** case, this peak exhibits a strong additional component at 1143 cm^{-1}. The peak at 1118 cm^{-1} is assigned to a helical conformation of the EG units and the

1143 cm^{-1} component to a nonhelical or trans conformation of the EG units (44, 45, 47, 48). This indicates that the **EG7** SAM adopts a highly ordered helical structure with very little disorder, with the **PEG5k** monolayer possessing a considerable amount of disorder. This is in agreement with the contact-angle and ellipsometry data presented above. Further evidence of the difference in the structural ordering of the two monolayers can be seen from the relative intensities of the vibrational modes of the terminal methoxy group. The vibrational modes of the methyl C−H stretching modes at 2981 and 2815 cm^{-1} and the CH_3 rocking mode at 1199 cm^{-1} are observable in the **EG7** spectrum, while in the **PEG5k** spectrum, these peaks are completely absent. This is again ascribed to the presence of an ordered structure in the **EG7** monolayer, exposing the terminal methoxy groups at a well-defined orientation with respect to the surface normal, whereas on the **PEG5k** sample, the methoxy groups adopt a random orientation with respect to the surface normal, leading to their intensity being too weak to be observed. IRRA intensities are a consequence of both the surface concentration of the adsorbed species and their relative orientations with respect to the surface. The difference in the surface grafting density alone is not sufficient to account for this huge difference in the intensity of these bands.

IR spectroscopic measurements carried out by exposing the samples to the two aqueous lubricants for the same duration as the tribological experiments did not show any noticeable degradation of the SAM films on this time scale (data not shown). However, it should be borne in mind that these ex situ measurements only served to check the stability of the films after exposure to lubricants with high salt concentrations and do not reflect the differences in the structure of the films in solution upon addition of the salts, as probed by the tribological and QCM-D measurements discussed below. To test such an effect of added salts on the chain conformations, it would require an in situ PM-IRRAS measurement of these films under high salt concentration, which is beyond the scope of the present investigation.

B. Aqueous Lubricating Properties in a Low-Salt Environment (HEPES 0). The lubricating properties of the SAM films were initially characterized in aqueous lubricants possessing virtually no salt (**HEPES 0**, ionic strength = 1 mM). Figure 4 shows the average values of three μ versus sliding speed experiments for both **PEG5k** and **EG7** SAMs in **HEPES 0**.

For both SAMs as well as for the uncoated Au substrate, the coefficients of friction (μ) were observed to increase gradually with decreasing sliding speed. At the highest sliding speeds, i.e., from 19 to 2.5 mm/s, the μ values obtained from all substrates were very similar. This feature is a characteristic of soft, hydrophilic tribological contacts in aqueous environments (49) and is thought to indicate the transition from soft elastohydrodynamic lubrication (soft EHL) to the mixed boundary−lubrication mechanism in the low-speed regime (50). Consistent with previous studies (34, 49), the relative difference in detailed surface chemical/

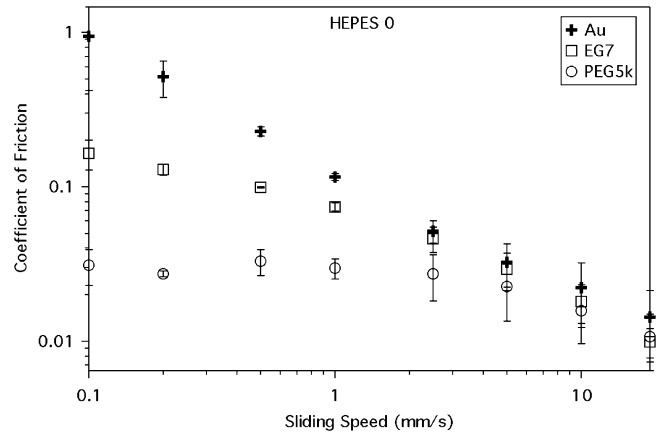

FIGURE 4. Coefficient of friction versus sliding speed plots obtained from sliding ox-PDMS pins against the two thiol SAMs on Au in HEPES 0. As a reference, an experiment with a bare Au substrate is included (normal load = 1 N).

conformational characteristics is more clearly reflected at slow sliding speeds, i.e., in the boundary−lubrication regime. Compared with bare Au substrates, both **EG7** and **PEG5k** SAMs show a significant reduction in the coefficient of friction at sliding speeds ≤1 mm/s. In the low-speed regime, the order in the friction coefficients was found to be proportional to that of the water contact angles (Table 1), i.e., $\mu_{Au} > \mu_{EG7} > \mu_{PEG5k}$. In contrast to **EG7** SAMs as well as to the uncoated Au surface, the μ values measured from **PEG5k** SAMs leveled off at 1 mm/s with friction coefficients in the range of 0.03. This observed low friction has mainly been ascribed to the "brushlike" conformation of the PEG chains in **PEG5k** SAMs, which allows for the generation of a hydration layer at the tribological interface (1, 4, 12, 49). Because of their well-ordered structure and consequent hydrophobic surface characteristics, the **EG7** SAMs cannot hold boundary−lubricant water films as effectively as **PEG5k** SAMs. In addition, the roughness of the **ox-PDMS** pin might have contributed to the observed frictional behavior. After oxidation, the Ra roughness of the pin was determined to be 7.8 nm over an area of 20 μm^2, as measured by AFM. However, it is believed that the significant film thickness of **PEG5k** monolayers (8.22 ± 1.77 nm in a dry state), which is comparable with the Ra roughness of the **ox-PDMS** pin, contributed to the low friction against the **ox-PDMS** pins in **HEPES 0**.

C. Influence of High Salt Concentrations on the Aqueous Lubricating Properties of SAMs: HEPES 0, 1 M NaCl. The influence of the salt concentration on the frictional response of the EG-based SAMs was investigated by testing **PEG5k** and **EG7** SAMs in **HEPES 0, 1 M NaCl** solutions (ionic strength = 1 M), while the speed range (19−0.1 mm/s) was identical to that used in the experiments performed in **HEPES 0**. In Figure 5a, we compare the μ versus revolution plots of individual measurements at a fixed sliding speed of 0.2 mm/s. For both **PEG5k** and **EG7** SAMs, a considerable increase in friction is observed in the high-salt solutions (**HEPES 0, 1 M NaCl**) compared to experiments in **HEPES 0**. Figure 5b compares the average μ values obtained from **PEG5k** and **EG7** SAMs

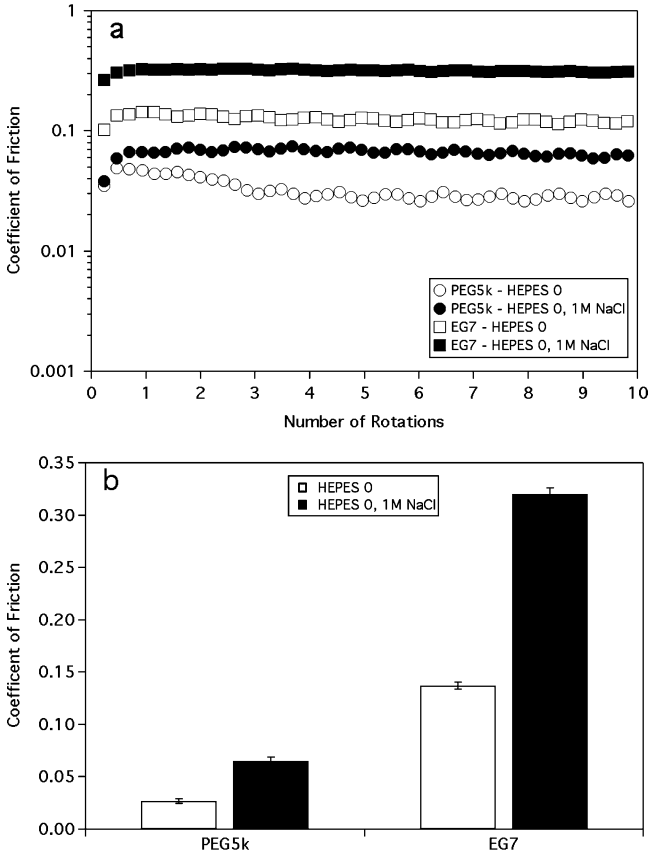

FIGURE 5. Coefficient of friction versus revolution plots from PEG5k and EG7 SAMs in HEPES 0 and HEPES 0, 1 M NaCl, measured at a sliding speed of 0.2 mm/s (a). Average μ values measured in low (HEPES 0) and high salt (HEPES 0, 1 M NaCl) solutions for both SAMs (b).

at a fixed sliding speed of 0.2 mm/s in low- and high-salt solutions. The relative increase in the coefficient of friction of about a factor of 2 in a 1 M NaCl solution is similar for both SAMs (**PEG5k**, $\mu \approx 0.03 \rightarrow \mu \approx 0.06$; **EG7**, $\mu \approx 0.15 \rightarrow \mu \approx 0.32$).

The higher friction in aqueous solutions with a high salt concentration is ascribed to the "salting-out" effect, which has frequently been reported for PEG molecules in aqueous salt solutions (18−23). This causes a reduction in hydration at the tribological interface comprised of end-tethered PEG chains and, consequently, leads to a degraded lubricating effect, as shown in Figure 5. For both **PEG5k** and **EG7** SAMs, we speculate that the interactions of salt with the two monolayers are similar in that the reduction in hydration leads to a less fluidlike layer. While the highly extended **PEG5k** SAMs are believed to collapse upon interaction with salts, we speculate that the helically ordered **EG7** SAMs can only become compressed to a certain extent because the oligo(ethylene glycol) SAMs are more densely packed compared to **PEG5k** films. It has been previously suggested (51) that **EG7** SAMs are capable of incorporating water within their structure and salting-out and/or cation complexation does occur to some extent. Because the helical structure of **EG7** SAMs is stabilized through hydrogen bonding with water molecules, it is believed that the presence of salts can induce the degradation of this highly ordered structure; first, hydrated ions can abstract water molecules that are involved

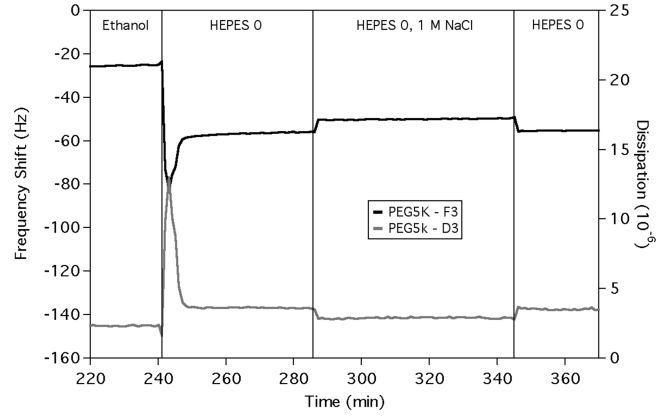

FIGURE 6. Frequency shift (PEG5k - F3) and dissipation changes (PEG5k - D3) in QCM-D experiments observed for PEG5k SAMs, which had been preadsorbed onto Au crystals from 50 μM ethanolic solutions. The induced changes occurred upon injection of different solvents.

in hydrogen bonding with EG units and, second, Na cations could penetrate into the **EG7** SAM to complex with ether O atoms. The second effect is proposed because the measured film thickness of the **EG7** SAMs was 30% below the theoretical all-trans thickness of **EG7** monolayers; i.e., the layer is not close-packed, and thus Na cations, whose dimensions are not significantly different from those of water, could readily penetrate into the layer and interact with EG units.

D. Influence of High Salt Concentration on the Conformation of Surface-Immobilized PEG SAMs. In order to understand the influence of salts on the conformation of end-tethered PEG chains (**PEG5k** SAM in this work) and, subsequently, to correlate this with their aqueous lubricating properties, QCM-D measurements were performed to elucidate the interaction of **PEG5k** monolayers with **HEPES 0** and **HEPES 0, 1 M NaCl**. Additionally, a reference experiment on a blank Au crystal was carried out because changes in the solvent properties (e.g., density, viscosity) can induce frequency shifts or dissipation changes on the uncoated QCM crystal.

Figure 6 shows resonance frequency (**PEG5k** - F3) as well as dissipation changes (**PEG5k** - D3) of the third overtone of a **PEG5k** monolayer that was preadsorbed from an ethanolic solution. The values measured from the reference crystal are subtracted from the displayed curves, and thus the presented frequency shifts and dissipation changes in Figure 6 are solely induced by the **PEG5k** SAM. Upon replacement of ethanol (adsorption medium) with **HEPES 0** at 240 min, an immediate frequency shift of −35 Hz and a change in dissipation of around 1×10^{-6} are observed for the third overtone of the quartz resonator. It is thus apparent that a significant hydration process is occurring upon injection of the aqueous lubricant, which indicates that a considerably higher amount of solvent is coupled to the adsorbed **PEG5k** SAM layer in the aqueous environment compared to ethanol. This is consistent with observations in previous studies (7, 8). The dissipation, which relates to the viscoelasticity of the adsorbed layer, also confirms that the **PEG5k** monolayers are highly solvated in water, judging from an increase in the dissipated energy upon switching from ethanol to **HEPES 0**.

After both frequency and dissipation signals had reached plateaus in **HEPES 0**, the high-salt aqueous lubricant (**HEPES 0, 1 M NaCl**) was injected (at ca. 285 min). Both frequency and dissipation changed immediately upon transition from **HEPES 0** (1 mM HEPES) to a high-salt-containing buffer; the effective increase in the frequency by 5−6 Hz indicates a decrease in the total mass coupled to the crystal in a high-ionic-strength environment. Similarly, dissipation of the SAM-bearing substrate decreased by 0.6×10^{-6}. In order to see whether the frequency shift is due to the loss of adsorbed PEG molecules on the surface or not, the **HEPES 0, 1 M NaCl** solution was again replaced with **HEPES 0** (at ca. 345 min), upon which the frequency and dissipation values returned to their initial magnitudes. Thus, the observed changes in QCM-D experiments are fully reversible and therefore solely induced by the high salt concentration.

Hence, the conformational change of PEG chains observed in 1 M NaCl solutions is basically similar to those in ethanolic solutions in that poorer solvency of a high-salt aqueous solution induces the loss of water within the monolayer and thus a partial collapse of the hydrated **PEG5k** brush. As mentioned in the Introduction, effects due to "salting-out" as well as complexation of cations with EG units have frequently been observed in various bulk properties of aqueous PEG solutions in high-ionic-strength media (18−22). The present observation confirms that such effects are at work for surface-tethered **PEG5k** SAMs. Ultimately, the reduction in hydration of the end-grafted polymer chains is thought to be mainly responsible for the poorer aqueous lubricating properties of **PEG5k** SAM films in the presence of high concentrations of NaCl.

QCM-D experiments on **EG7** SAMs were also carried out but are not shown. The oligo(ethylene glycols) with a 14× lower molecular weight than **PEG5k** molecules only induced frequency shifts of 2−4 Hz upon adsorption from ethanol. Thus, the sensitivity of the QCM-D setup was insufficiently high to follow changes in the hydration properties of **EG7** SAMs with or without 1 M NaCl.

CONCLUSIONS

We have demonstrated in this work that surface-grafted PEG chains in aqueous solution display reduced hydration and increased interfacial friction forces upon the addition of a high-concentration salt (1 M NaCl), as confirmed by means of QCM-D and pin-on-disk tribometry, respectively. This behavior is consistent with the well-documented effect of electrolytes on various bulk properties of aqueous PEG solutions, such as reduced viscosity and lowered cloud-point temperature, arising from "salting-out" effects. Experimental verification of the "salting-out" effect for surface-grafted PEG layers was obtained in this work by employing thiolated PEG SAMs on Au substrates, which show no change in the surface density of PEG chains upon the addition of salts. In addition, pin-on-disk tribometry with a soft slider (oxidized PDMS) allows for a nondestructive probing of the tribological properties of the surface-grafted PEG layers upon the addition of salts. The degraded aqueous lubricating properties of surface-grafted PEG layers upon the addition of high-concentration salts are mainly ascribed to the conformational changes of the PEG chains, which are indicated by their reduced hydration.

REFERENCES AND NOTES

(1) Lee, S.; Spencer, N. D. In *Superlubricity*; Erdemir, A., Martin, J.-M., Eds.; Elsevier: New York, 2007; pp 365−396.
(2) Klein, J. *Annu. Rev. Mater. Sci.* **1996**, *26*, 581–612.
(3) Grest,G. S. *Polymers in Confined Environments*, 1st ed.; Springer: New York, 1999; Vol. 138, pp 149183.
(4) Lee, S.; Spencer, N. D. *Science* **2008**, *319*, 575–576.
(5) Schorr, P. A.; Kwan, T. C. B.; Kilbey, S. M.; Shaqfeh, E. S. G.; Tirrell, M. *Macromolecules* **2003**, *36*, 389–398.
(6) Limpoco, F. T.; Advincula, R. C.; Perry, S. S. *Langmuir* **2007**, *23*, 12196–12201.
(7) Muller, M. T.; Yan, X. P.; Lee, S. W.; Perry, S. S.; Spencer, N. D. *Macromolecules* **2005**, *38*, 5706–5713.
(8) Muller, M. T.; Yan, X. P.; Lee, S. W.; Perry, S. S.; Spencer, N. D. *Macromolecules* **2005**, *38*, 3861–3866.
(9) O'Shea, S. J.; Welland, M. E.; Rayment, T. *Langmuir* **1993**, *9*, 1826–1835.
(10) Overney, R. M.; Leta, D. P.; Pictroski, C. F.; Rafailovich, M. H.; Liu, Y.; Quinn, J.; Sokolov, J.; Eisenberg, A.; Overney, G. *Phys. Rev. Lett.* **1996**, *76*, 1272–1275.
(11) Forster, A. M.; Kilbey, S. M. Influence of shearing parameters on the frictional forces measured between polymer brushes. 225th National Meeting of the American Chemical Society, New Orleans, LA, 2003.
(12) Drobek, T.; Spencer, N. D. *Langmuir* **2008**, *24*, 1484–1488.
(13) Raviv, U.; Frey, J.; Sak, R.; Laurat, P.; Tadmor, R.; Klein, J. *Langmuir* **2002**, *18*, 7482–7495.
(14) Pettersson, T.; Naderi, A.; Makuska, R.; Claesson, P. M. *Langmuir* **2008**, *24*, 3336–3347.
(15) Sofia, S. J.; Premnath, V.; Merrill, E. W. *Macromolecules* **1998**, *31*, 5059–5070.
(16) Kenausis, G. L.; Voros, J.; Elbert, D. L.; Huang, N. P.; Hofer, R.; Ruiz-Taylor, L.; Textor, M.; Hubbell, J. A.; Spencer, N. D. *J. Phys. Chem. B* **2000**, *104*, 3298–3309.
(17) Unsworth, L. D.; Sheardown, H.; Brash, J. L. *Langmuir* **2008**, *24*, 1924–1929.
(18) Bailey, F. E.; Callard, R. W. *J. Appl. Polym. Sci.* **1959**, *1*, 56–62.
(19) Bailey, F. E.; Koleske, J. V. *Poly(ethylene oxide)*; Academic Press: New York, 1976.
(20) Lundberg, R. D.; Bailey, F. E.; Callard, R. W. *J. Polym. Sci., Part A: Polym. Chem.* **1966**, *4*, 1563.
(21) Ataman, M. *Colloid Polym. Sci.* **1987**, *265*, 19–25.
(22) Boucher, E. A.; Hines, P. M. *J. Polym. Sci., Part B: Polym. Phys.* **1976**, *14*, 2241–2251.
(23) Briscoe, B.; Luckham, P.; Zhu, S. *Macromolecules* **1996**, *29*, 6208–6211.
(24) Tasaki, K. *Comput. Theor. Polym. Sci.* **1999**, *9*, 271–284.
(25) Masuda, Y.; Nakanishi, T. *Colloid Polym. Sci.* **2002**, *280*, 547–553.
(26) Pedersen, C. J. *J. Am. Chem. Soc.* **1967**, *89*, 7017.
(27) Frensdor, H. K. *J. Am. Chem. Soc.* **1971**, *93*, 600.
(28) Florin, E.; Kjellander, R.; Eriksson, J. C. *J. Chem. Soc., Faraday Trans. 1* **1984**, *80*, 2889–2910.
(29) Bjorling, M.; Karlstrom, G.; Linse, P. *J. Phys. Chem.* **1991**, *95*, 6706–6709.
(30) Lee, S.; Muller, M.; Heeb, R.; Zurcher, S.; Tosatti, S.; Heinrich, M.; Amstad, F.; Pechmann, S.; Spencer, N. D. *Tribol. Lett.* **2006**, *24*, 217–223.
(31) Nichols, A.; Street, S. C. *Analyst* **2001**, *126*, 1269–1273.
(32) Nakano, M.; Ishida, T.; Numata, T.; Ando, Y.; Sasaki, S. *Jpn. J. Appl. Phys., Part 1* **2003**, *42*, 4734–4738.
(33) Masuko, M.; Miyamoto, H.; Suzuki, A. *Tribol. Int.* **2007**, *40*, 1587–1596.
(34) Lee, S.; Heeb, R.; Venkataraman, N. V.; Spencer, N. D. *Tribol. Lett.* **2007**, *28*, 229–239.
(35) Xiao, X. D.; Hu, J.; Charych, D. H.; Salmeron, M. *Langmuir* **1996**, *12*, 235–237.
(36) Lio, A.; Charych, D. H.; Salmeron, M. *J. Phys. Chem. B* **1997**, *101*, 3800–3805.
(37) Yang, X. J.; Perry, S. S. *Langmuir* **2003**, *19*, 6135–6139.
(38) Brewer, N. J.; Beake, B. D.; Leggett, G. J. *Langmuir* **2001**, *17*, 1970–1974.

(39) Shon, Y. S.; Lee, S.; Colorado, R.; Perry, S. S.; Lee, T. R. *J. Am. Chem. Soc.* **2000**, *122*, 7556–7563.
(40) Sung, I. H.; Kim, D. E. *Tribol. Lett.* **2004**, *17*, 835–844.
(41) Ahn, H. S.; Cuong, P. D.; Park, S.; Kim, Y. W.; Lim, J. C. *Wear* **2003**, *255*, 819–825.
(42) Rodahl, M.; Hook, F.; Krozer, A.; Brzezinski, P.; Kasemo, B. *Rev. Sci. Instrum.* **1995**, *66*, 3924–3930.
(43) Hook, F.; Rodahl, M.; Brzezinski, P.; Kasemo, B. *Langmuir* **1998**, *14*, 729–734.
(44) Vanderah, D. J.; Arsenault, J.; La, H.; Gates, R. S.; Silin, V.; Meuse, C. W.; Valincius, G. *Langmuir* **2003**, *19*, 3752–3756.
(45) Vanderah, D. J.; Valincius, G.; Meuse, C. W. *Langmuir* **2002**, *18*, 4674–4680.
(46) Unsworth, L. D.; Tun, Z.; Sheardown, H.; Brash, J. L. *J. Colloid Interface Sci.* **2005**, *281*, 112–121.
(47) Malysheva, L.; Onipko, A.; Liedberg, B. *J. Phys. Chem. A* **2008**, *112*, 728–736.
(48) Tokumitsu, S.; Liebich, A.; Herrwerth, S.; Eck, W.; Himmelhaus, M.; Grunze, M. *Langmuir* **2002**, *18*, 8862–8870.
(49) Lee, S.; Spencer, N. D. *Tribol. Int.* **2005**, *38*, 922–930.
(50) Moore, D. F. *Wear* **1975**, *35*, 159–170.
(51) Clark, S. L.; Montague, M. F.; Hammond, P. T. *Macromolecules* **1997**, *30*, 7237–7244.

AM900062H